0026-895X/08/7401-101–108$20.00
MOLECULAR PHARMACOLOGY
Copyright © 2008 The American Society for Pharmacology and Experimental Therapeutics
Mol Pharmacol 74:101–108, 2008

Vol. 74, No. 1
44834/3357609
Printed in U.S.A.

RNA Interference-Mediated Knockdown of Dynamin 2 Reduces Endocannabinoid Uptake into Neuronal dCAD Cells

Matthew J. McFarland, Tamera K. Bardell, Marla L. Yates, Ekaterina A. Placzek, and Eric L. Barker

Department of Medicinal Chemistry and Molecular Pharmacology, Purdue University, West Lafayette, Indiana

Received January 3, 2008; accepted April 23, 2008

ABSTRACT

The precise mechanism by which the cellular uptake of the endocannabinoid anandamide (AEA) occurs has been the source of much debate. In the current study, we show that neuronal differentiated CAD (dCAD) cells accumulate anandamide by a process that is inhibited in a dose-dependent manner by *N*-(4-hydroxyphenyl)arachidonylamide (AM404). We also show that dCAD cells express functional fatty acid amide hydrolase, the enzyme primarily responsible for anandamide metabolism. Previous data from our laboratory indicated that anandamide uptake occurs by a caveolae-related endocytic mechanism in RBL-2H3 cells. In the current study, we show that anandamide uptake by dCAD cells may also occur by an endocytic process that is associated with detergent-resistant membrane microdomains or lipid rafts. Nystatin and progesterone pretreatment of dCAD cells significantly inhibited anandamide accumulation. Furthermore, RNA interference (RNAi)-mediated knockdown of dynamin 2, a protein involved in endocytosis, blocked the internalization of the fluorescently labeled anandamide analog SKM 4-45-1 ([3′,6′-*bis*(acetyloxy)-3-oxospiro[isobenzofuran-1(3*H*),9′-[9*H*]xanthen-5-yl]-2-[[1-oxo-5*Z*,8*Z*,11*Z*,14*Z*-eicosatetraenyl]amino]ethyl ester carbamic acid). RNAi-mediated knockdown of the β2 subunit of the clathrin-associated activator protein 2 complex had no effect on SKM 4-45-1 internalization. We were surprised to find that dynamin 2 knockdown in dCAD cells did not affect [^{3}H]AEA uptake. However, dynamin 2 knockdown caused a significant increase in the overall levels of intact [^{3}H]AEA associated with the cells, suggesting that trafficking of [^{3}H]AEA to FAAH had been disrupted. This finding may be the result of an accumulation of the anandamide carrier protein in detergent-resistant membranes after dynamin 2 knockdown. Our studies provide evidence that the cellular uptake of anandamide may occur by a dynamin 2-dependent, caveolae-related endocytic process in dCAD cells.

The endocannabinoid anandamide (AEA) is an agonist of the cannabinoid 1 and 2 receptors (Matsuda et al., 1990; Munro et al., 1993) and some vanilloid type ion channels (Di Marzo et al., 2001; Voets and Nilius, 2003). AEA is internalized by most cell types and is thought to be metabolized primarily by the intracellular enzyme fatty acid amide hydrolase (FAAH) (Deutsch and Chin, 1993; Di Marzo et al., 1994; Cravatt et al., 1996). Previous studies from our laboratory have indicated that AEA uptake potentially occurs by a caveolae-related, or clathrin-independent, endocytic process (McFarland et al., 2004). Interestingly, neurons are not thought to express caveolin-1 but do exhibit lipid raft-related endocytic processes (Cameron et al., 1997). Thus, our studies seek to validate a neuronal-like cell line as a useful model in the study of AEA uptake and to show that AEA uptake can be disrupted by using molecular inhibitors that are specifically targeted to endocytic processes.

Cath.a cells display neuronal properties and express pan-neuronal markers but lack classic neuronal morphology (Suri et al., 1993; Lazaroff, 1996). Cath.a differentiated (CAD) cells are derived from the Cath.a cell line and are characterized by the loss of the immortalizing oncogene present in Cath.a cells (Qi et al., 1997). CAD cells also undergo a reversible morphological differentiation that is initiated when serum is removed from the cell culture media (Qi et al., 1997). Differentiated CAD (dCAD) cells stop proliferating and extend long neuronal processes characteristic of primary neuronal cell cultures (Qi et al., 1997). Accompanying the morphological

This works supported by National Institutes of Health grants R21-DA13268 and R21-DA018844 (to E.L.B.).
Article, publication date, and citation information can be found at http://molpharm.aspetjournals.org.
doi:10.1124/mol.108.044834.

ABBREVIATIONS: AEA, anandamide; FAAH, fatty acid amide hydrolase; CAD, Cath.a differentiated; cCAD, cycling CAD; siRNA, short interfering RNA; AP, activator protein; Dyn 2, dynamin 2; KRH, Krebs-Ringer-HEPES; AM404, *N*-(4-hydroxyphenyl)arachidonylamide; PBS, phosphate-buffered saline; MAFP, methyl arachidonyl fluorophosphonate; RNAi, RNA interference; 488-CT, cholera toxin B subunit-conjugated Alexa Fluor 488; 488-Tf, transferrin-conjugated Alexa Fluor 488; TLC, thin layer chromatography; CB, cannabinoid; NP, nystatin/progesterone; SKM 4-45-1, ([3′,6′-*bis*(acetyloxy)-3-oxospiro[isobenzofuran-1(3*H*),9′-[9*H*]xanthen-5-yl]-2-[[1-oxo-5*Z*,8*Z*,11*Z*,14*Z*-eicosatetraenyl]amino]ethyl ester carbamic acid).

differentiation of CAD cells is an observed change in the expression and function of several neuronal proteins. For example, dCAD cells express higher levels of tyrosine hydroxylase (Lazaroff et al., 1998) and somatostatin receptor subtype 2a (Hashemi et al., 2003), exhibit a decrease in sodium current accompanied by an increase in potassium current (Wang and Oxford, 2000), and display alterations in cyclic AMP-mediated signaling (Hashemi et al., 2003). Despite reported differences in their cellular signaling and protein expression profiles, both cycling CAD (cCAD) and dCAD cells express neuron-specific proteins and display the biochemical characteristics of neuronal cells (Qi et al., 1997).

In RBL-2H3 cells, AEA transport occurs via a clathrin-independent, or caveolae-related endocytic process, substantiated by studies using pharmacological inhibitors of endocytosis (McFarland et al., 2004). We tested the hypothesis that the disruption of lipid rafts/detergent-resistant membranes in dCAD cells would also decrease the cellular accumulation of AEA to confirm that endocytosis may play a role in AEA uptake in neuronal cells. To avoid the potential problems associated with biochemical disruption of lipid rafts, we examined AEA uptake in dCAD cells after treatment with short interfering RNA (siRNA) to knockdown expression of the β2 subunit of the AP2 complex, a protein necessary for clathrin-mediated endocytosis (Huang et al., 2004), as well as dynamin 2 (Dyn 2), a protein involved in both clathrin-mediated and clathrin-independent endocytic processes (Altschuler et al., 1998; Maxfield and McGraw, 2004). The results of our studies are consistent with a role for endocytosis in the neuronal uptake of endocannabinoids.

Materials and Methods

Cell Culture. cCAD cells were maintained in a 1:1 ratio of Ham's F-12/Dulbecco's modified Eagle's medium with 5% bovine calf serum and 5% fetal clone 1 supplemented with 1% penicillin/streptomycin, and 2 mM L-glutamine. Cells were grown in a humidified environment containing 5% CO_2 and held at the constant temperature of 37°C. cCAD cells were maintained in serum-free 1:1 Ham's F-12/Dulbecco's modified Eagle's medium and were allowed to differentiate for 36 h before experiments to generate dCAD cells.

[^{3}H]AEA Uptake and SKM 4-45-1 Internalization Assays. CAD cells were plated at approximately 50,000 cells per well in 24-well culture dishes and then allowed to differentiate in serum-free media for 36 h. The resulting dCAD cells were then transfected with siRNA oligonucleotides as described below. After the transfection period, media were removed and 1 nM [^{3}H]AEA (labeled on the arachidonate portion of the molecule; PerkinElmer Life and Analytical Sciences, Waltham, MA) in Krebs-Ringer-HEPES (KRH) buffer (120 mM NaCl, 4.7 mM KCl, 2.2 mM $CaCl_2$, 10 mM HEPES, 1.2 mM KH_2PO_4, and 1.2 mM $MgSO_4$, pH 7.4) was added to all samples and allowed to incubate for 5 min at 37°C. To determine the effects of cholesterol depletion on AEA accumulation in dCAD cells, uptake assays were performed after a 30-min incubation in KRH buffer containing nystatin (25 μg/ml) and progesterone (10 μg/ml). Control cells were incubated for 30 min in 1× KRH buffer. AM404 (100 μM) was used to define nonspecific uptake and was added 10 min before the addition of [^{3}H]AEA at 37°C. Cells were then washed once with 1× KRH buffer containing 1% bovine serum albumin, and MicroScint-20 (PerkinElmer Life and Analytical Sciences) was added to each well. The amount of tritium present was determined using a TopCount microplate scintillation and luminescence counter (PerkinElmer Life and Analytical Sciences). To verify morphological changes, cells were seeded in clear 24-well tissue culture plates for uptake assays in untransfected dCAD cells. To quantify tritium from the wells of clear plates, cells were solubilized in 1% SDS and transferred to vials containing 10 ml of EcoLite scintillation fluid (MP Biomedicals, Irvine, CA) for subsequent scintillation counting. For experiments examining SKM 4-45-1 internalization, CAD cells were treated with SKM 4-45-1 (25 μM) and increasing concentrations of AM404 for 10 min in prewarmed 37°C buffer. Fluorescence was quantified using a FUSION microplate reader (PerkinElmer Life and Analytical Sciences).

Determination of Plasma Membrane Cholesterol Content. Membrane cholesterol content was determined according to a method described previously (Millard et al., 2005). CAD cells were plated in triplicate at 5×10^4 cells per 35-mm well in complete culture medium. Twenty-four hours later, cells were washed three times with PBS and then incubated in complete medium that had been supplemented with 10% lipoprotein-deficient fetal calf serum and 1 μCi/ml [^{3}H]cholesterol (40 Ci/mmol; GE Healthcare, Chalfont St. Giles, UK). Cells were labeled to equilibrium for 48 h. Cells were then washed three times with PBS and then treated with nystatin/progesterone as described above. Membrane cholesterol was extracted by a 10 min incubation with medium containing 4% methyl-β-cyclodextrin. Media was collected, cells were washed three times with PBS, and proteins were extracted. Protein concentrations were determined using the bicinchoninic acid assay. [^{3}H]Cholesterol extracted into the medium was quantified by scintillation counting and normalized to total protein values.

FAAH Activity Assays. FAAH activity was determined by a modification of a previously published method (Day et al., 2001). In brief, CAD cells were homogenized in buffer containing 20 mM Tris-HCl, 1 mM EDTA, 0.7 μg/ml pepstatin A, and 0.5 μg/ml leupeptin. Cell homogenates were then incubated with 5 nM [^{3}H]AEA [ethanolamine 1-^{3}H] (ARC, St. Louis, MO) in the presence or absence of 500 nM methyl arachidonyl fluorophosphonate (MAFP) with a reaction volume of 250 μl. After the incubation, the reaction was terminated by adding 500 μl of 1:1 chloroform/methanol (2× assay volume) to each tube. Samples were vortexed for 30 s and centrifuged at 3900*g* for 1 min to separate the aqueous and organic phases. Then, 100-μl aliquots were collected from both the aqueous and organic phases, and radioactivity was quantified using a TopCount Microplate scintillation and luminescence counter (PerkinElmer Life and Analytical Sciences). The [^{3}H]AEA used in these experiments was labeled on the ethanolamine portion of the molecule and not the arachidonate backbone; therefore, as FAAH activity increased so did the level of radioactivity in the aqueous phase.

Western Blot Analysis. Western blot analysis was performed as described previously (McFarland et al., 2004). The presence of FAAH, dynamin 2, and the β2 subunit of the AP2 complex was detected using rabbit polyclonal anti-FAAH, rabbit polyclonal anti-dynamin 2 (Abcam Inc., Cambridge, MA), and mouse monoclonal anti-β2 subunit (Novus Biologicals, Inc., Littleton, CO) primary antibodies, respectively, followed by an incubation with horseradish peroxidase-labeled goat anti-rabbit or goat anti-mouse secondary antibodies (Bio-Rad Laboratories, Hercules, CA), and enhanced chemiluminescence detection reagents. Membranes were then exposed to X-ray film.

RNAi Transfections. CAD cells were transfected with siRNA oligonucleotides (Stealth RNAi; Invitrogen, Carlsbad, CA) directed against either Dyn2 or the β2 subunit of the AP2 complex mRNA using the Lipofectamine 2000 (Invitrogen) RNAi transfection protocol for mammalian cells provided by Invitrogen (16 pmol of each siRNA oligo was added for every 1 μl of Lipofectamine 2000 used). For later experiments, the siLentFect Lipid Reagent was used following the manufacturer's protocol (Bio-Rad Laboratories). Protein knockdown was achieved by cotransfection of two different siRNA oligonucleotides targeted at each individual protein. The siRNA sequences were as follows: Dyn 2: NM_007871_stealth_1410, GUGGACCUGGUUAUCCAGGAGCUAA, and NM_007871_stealth_2009, GGCAGAGAAUGAGGAUGGAGCACAA, β2/AP2: NM_027915_

stealth_1591, GCUGGUCCAACAGGUCUUGAGCUUA, and NM_027915_stealth_2400, CCAUACAUACUCCACUGAUGCCAAA.

Stealth RNAi negative control duplex was purchased from Invitrogen. Sequences of the negative (mock) control contained medium GC content and matched no known mRNA sequence in the vertebrate genome.

Confocal Microscopy. dCAD cells plated in a four-well Lab-Tek Chambered Coverglass slide (Nalge Nunc International, Rochester, NY) were transfected with the appropriate siRNA oligonucleotides. Then, 72 h after transfection, the cells were treated with the B subunit of cholera toxin conjugated to Alexa Fluor 488 (488-CT) (Invitrogen), transferrin conjugated to Alexa Fluor 488 (488-Tf) (Invitrogen), or SKM 4-45-1 (Muthian et al., 2000) for 10 min and imaged using oil immersion confocal microscopy at 60× magnification with a krypton (488 nm)/argon (568 nm) laser, band pass filter at 522 to 535 nm, and a long pass filter at 588 nm.

Thin Layer Chromatography Analysis for Intact [^{3}H]AEA. dCAD cells transfected with either mock or dynamin 2-targeted siRNA were treated with [^{3}H]AEA (1 nM) for 5 min and washed three times with KRH containing 1% bovine serum albumin. After the removal of the wash buffer, transfected dCAD cells were exposed to 1 ml of lysis buffer (0.5% Triton X-100, 50 mM Tris-HCl, 150 mM NaCl, and 5 mM EDTA) on ice for 20 min. The cells were then scraped and added to a 15-ml centrifuge tube kept on ice that contained 1.5 ml of 2:1 $CHCl_3$/MeOH (v/v) and 8 μl of 1 M HCl. The aqueous and organic phases were mixed by vortexing and then separated by centrifugation (3000*g* for 15 min at 4°C). The organic layer was removed from each sample, placed in a clean glass tube, and 1 ml of ice-cold $CHCl_3$ was added to the remaining aqueous layer. The phases were again mixed by vortexing and separated by centrifugation (3000*g* for 15 min at 4°C). The resulting organic layer was removed and combined with the previously extracted organic layer. The solvent from the sample was evaporated under a stream of argon. The tubes were capped and kept overnight at −20°C. The concentrated samples were resuspended in 52 μl of ice-cold $CHCl_3$ and then divided into two spots of 20 μl each onto 20- × 20-cm glass-backed silica gel thin layer chromatography (TLC) plates. The mobile phase in which the TLC plates were developed consisted of 11:5 ethyl acetate/isooctane saturated with H_2O and acetic acid. After the plates were dried, the lipids were visualized with iodine vapor. The location of the [^{3}H]AEA spot was identified by comparison with the unlabeled AEA standard. The silica corresponding to the AEA spots was then scraped off of the TLC plate into scintillation vials and allowed to equilibrate for 72 h in scintillation fluid. Radioactivity was then quantified by liquid scintillation counting.

Results

Endocannabinoid Uptake Properties of dCAD and cCAD Cells. Differentiated and undifferentiated CAD (dCAD and cCAD, respectively) cells displayed robust uptake of radiolabeled anandamide. The accumulation of AEA by CAD cells was inhibited by the AEA uptake inhibitor AM404, with a K_i value in the low micromolar to high nanomolar range (Fig. 1A). SKM 4-45-1 is a fluorescent analog of AEA (Muthian et al., 2000). Previous results using AM404 indicate that SKM 4-45-1 is internalized by the same mechanism as AEA in C6 glioma cells (Muthian et al., 2000). SKM 4-45-1 internalization in CAD cells was also inhibited by AM404, with K_i values similar to those previously reported for inhibition of [^{3}H]AEA uptake (Fig. 1B) (Muthian et al., 2000). Furthermore, Western blot analysis of whole cell lysates from dCAD and cCAD cells revealed that both cell types express the AEA-metabolizing enzyme FAAH (Fig. 2A). FAAH activity assays performed on CAD cell homogenates revealed FAAH activity that was inhibited in the presence of the FAAH inhibitor MAFP (Fig. 2B). FAAH has been implicated in playing an important role in AEA uptake (Day et al., 2001; Glaser et al., 2003). We were surprised to find that although FAAH was present in CAD cells, inhibition of FAAH by phenylmethylsulfonyl fluoride did not reduce AEA uptake in CAD cells (data not shown). This finding suggests that FAAH may not contribute to AEA uptake in these neuronal cells.

Effect of Nystatin/Progesterone Pretreatment on AEA Uptake. As described above, both cCAD and dCAD cells display endocannabinoid properties. However, dCAD cells are morphologically similar to primary neuronal cell cultures. Thus, dCAD cells were used for our additional studies to assess the role that endocytosis might play in the AEA uptake by a neuronal cell line. dCAD cells were treated with nystatin and progesterone to deplete membrane cholesterol levels and thereby disrupt detergent-resistant lipid raft domains. Based on the results from previous studies with RBL-2H3 cells (McFarland et al., 2004), we expected that this treatment would decrease the specific uptake of AEA by dCAD cells. Indeed, the disruption of detergent-resistant membrane microdomains in dCAD cells resulted in an ~50% decrease in the specific uptake of [^{3}H]AEA (Fig. 3). Control experiments confirmed that nystatin and progesterone treat-

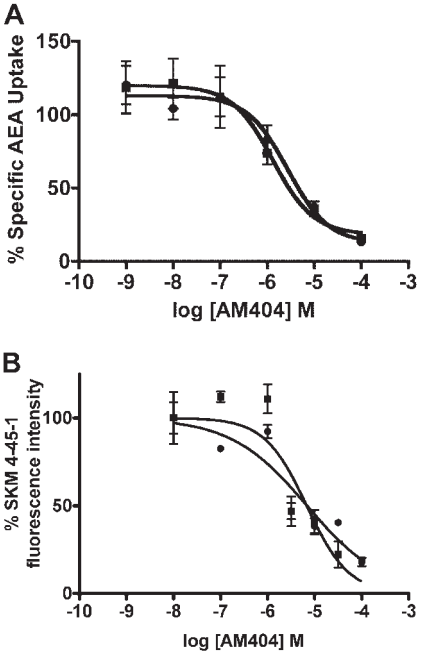

Fig. 1. Dose-dependent inhibition of AEA uptake and SKM 4-45-1 internalization by AM404. Both dCAD (■) and cCAD (circf) cells were treated with increasing concentrations of AM404 for 10 min at 37°C. A, after the incubation with AM404, [^{3}H]AEA was added at a final concentration of 1 nM as described under *Materials and Methods*. Data shown are means ± S.E.M. and are representative of four separate experiments performed in triplicate. K_i values (means ± S.E.M.; n = 3) were 850 ± 600 nM (cCAD) and 930 ± 150 nM (dCAD). The cpm values for cCAD cells were total = 6440 ± 914 and nonspecific = 850 ± 86. The cpm values for dCAD cells were total = 5124 ± 1456 and nonspecific = 794 ± 35. B, cells were treated with SKM 4-45-1 (25 μM) and increasing concentrations of AM404 for 10 min, and fluorescence was determined on a FUSION microplate reader (PerkinElmer Life and Analytical Sciences). IC_{50} values were converted to K_i values using the Cheng-Prusoff equation (K_m value for SKM 4-45-1 = 16 μM). K_i values (means ± S.E.M.; n = 3) were 24 ± 12 μM (cCAD) and 16 ± 10 μM (dCAD). Data shown are representative of three separate experiments performed in duplicate. Arbitrary fluorescence unit values for cCAD cells were total = 13,858 ± 1856, nonspecific = 7521 ± 573, and background = 4313 ± 625. Arbitrary fluorescence unit values for dCAD cells were total = 23,137 ± 6590, nonspecific = 11,309 ± 4024, and background = 2006 ± 74.

ment reduced membrane cholesterol by approximately 50%, consistent with the effect on [^{3}H]AEA uptake (Fig. 3, inset).

RNAi-Mediated Knockdown of Endocytic Machinery. The studies described above with cholesterol depletion, along with our previous work (McFarland et al., 2004), suggested that AEA uptake occurs via a caveolae-related endocytic process. The nonspecific nature of the cholesterol depletion treatments limits interpretation of our results.

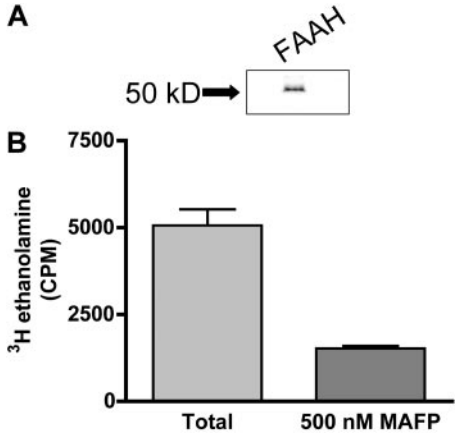

Fig. 2. Expression of FAAH in CAD cells. A, cCAD and dCAD cells express FAAH. Western blots were performed as described under *Materials and Methods*. Data are representative of three separate experiments. B, cCAD and dCAD cells were homogenized and then incubated at 37°C for 10 min. Cell homogenates were then incubated with 5 nM [^{3}H]AEA in the presence or absence of 500 nM MAFP. After the incubation, the reaction was terminated, and the aqueous and organic phases were separated. Bars represent AEA-derived [^{3}H]ethanolamine present in the aqueous phase (i.e., metabolized AEA) after the termination of the reaction as a direct measure of FAAH activity. Data shown are means ± S.D. of three separate experiments performed in duplicate.

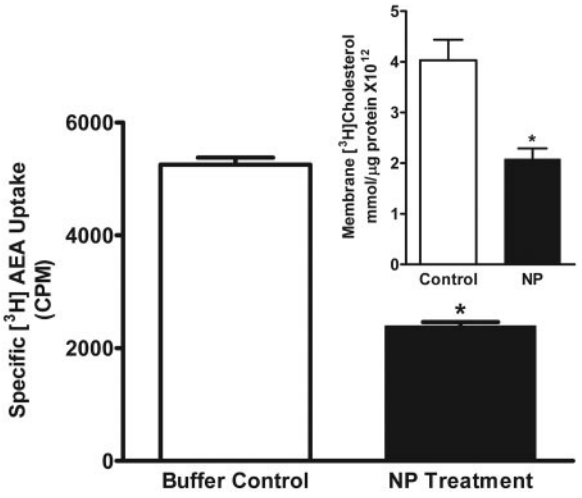

Fig. 3. Effect of lipid raft disruption on AEA uptake in dCAD cells. dCAD cells were pretreated for 30 min with 25 μg/ml nystatin and 10 μg/ml progesterone (NP treatment). After NP treatment, AEA uptake assays were performed in 1× KRH at 37°C in the presence or absence of 100 μM AM404 to define nonspecific transport. Transport assays were performed for 5 min with 1 nM [^{3}H]AEA as described under *Materials and Methods*. Data are means ± S.E.M. combined from three separate experiments performed in triplicate. The cpm values for control cells were total = 5755 ± 118 and nonspecific = 502 ± 41. The cpm values for NP-treated cells were total = 3117 ± 40 and nonspecific = 729 ± 61. Inset, effect of NP treatment on membrane cholesterol content. Cholesterol content in CAD cell membranes was determined as described under *Materials and Methods*. Data are means ± S.E.M. from two separate experiments performed in triplicate. *, $p < 0.05$.

Therefore, we assessed the role of clathrin-independent versus clathrin-dependent endocytosis of AEA in dCAD cells using molecular inhibitors. Specifically, we used an RNAi approach to knockdown expression of either the β2 subunit of the AP2 complex or dynamin 2. Knockdown of the β2 subunit of the AP2 complex should only inhibit clathrin-mediated endocytosis and have no effect on clathrin-independent, or caveolae-related, endocytic processes (Johannes and Lamaze, 2002; Huang et al., 2004). Dynamin 2, however, is a GTPase that has been shown to play a role in both clathrin-mediated and clathrin-independent endocytosis (Altschuler et al., 1998; Maxfield and McGraw, 2004). After transfection with siRNA oligonucleotides using Lipofectamine 2000 (Invitrogen), the cells were incubated for 72 h to allow for the degradation of resident protein. Western blot analysis confirmed that we had successfully reduced the expression of both proteins by 70 to 90% (Fig. 4). Control transfection experiments using green fluorescent protein (pEGFP-N1; Clontech, Mountain View, CA) confirmed transfection efficiency in CAD cells to be greater than 80% (data not shown), consistent with our observed knockdown effects.

To verify the effects of both β2 subunit and dynamin 2 knockdown, we used the Alexa Fluor 488-conjugated probes transferrin (488-Tf) and the B subunit of cholera toxin (488-CT), which are endocytosed by clathrin-dependent and lipid raft/caveolae-related endocytic processes, respectively. As was expected, after a 10-min treatment with either probe at 37°C, RNAi knockdown of the β2 subunit of the AP2 complex significantly reduced the internalization of 488-Tf (Fig. 5) but had no effect on 488-CT endocytosis in dCAD cells compared with control (Fig. 6). In the case of dynamin 2, RNAi knockdown inhibited internalization of *both* 488-Tf (Fig. 5) and 488-CT (Fig. 6) in dCAD cells. These control experiments confirm that by knocking down expression of the β2 subunit of the AP2 complex we are only inhibiting clathrin-mediated endocytosis (i.e., 488-Tf internalization), whereas knockdown of dynamin 2 inhibits both clathrin-dependent endocytosis as well as a lipid raft-related endocytic process that is clathrin-independent.

AEA Uptake after RNAi Transfection. Our results above showing AM404 inhibition of both [^{3}H]AEA and SKM 4-45-1 internalization (Fig. 1) suggest that both compounds are transported by a common process in the CAD cells. Because the fluorescence associated with SKM 4-45-1 is only observed after internalization of the compound, it is a true marker of actual uptake into the cell (Muthian et al., 2000). To assess the effects that RNAi knockdown of endocytic machinery might have on

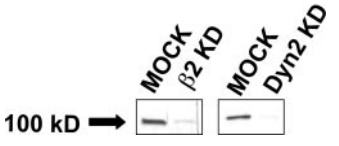

Fig. 4. RNAi-mediated knockdown of the β2 subunit of the AP2 complex and dynamin 2. dCAD cells were transfected with Stealth RNAi (Invitrogen) using Lipofectamine 2000 (Invitrogen) and then incubated at 37°C in serum-free media for 72 h to allow for protein degradation. The expression of both the β2 subunit of the AP2 complex and the protein dynamin 2 was decreased by >90% compared with mock siRNA (nonsense sequence) transfection. siRNA oligonucleotides had no effect on the level of control protein β-actin (data not shown). To control for protein loading, equal amounts of total protein (20 μg) from the cell lysates were added to each well for Western blot analysis as described under *Materials and Methods*. Both proteins resolved at the expected molecular weights. Data are representative of three separate experiments.

AEA uptake, cells were treated with 25 μM SKM 4-45-1 at 37°C for 10 min after knockdown of the expression of either the β2 subunit of the AP2 complex or dynamin 2. Compared with control, RNAi knockdown of the β2 subunit of the AP2 complex caused no observable change in the internalization of SKM 4-45-1 (Fig. 7). However, knockdown of dynamin 2 expression abolished the SKM 4-45-1 fluorescence accumulation in dCAD cells (Fig. 7).

In addition to examining SKM 4-45-1 accumulation, we investigated the effects of RNAi-mediated knockdown of both the β2 subunit of the AP2 complex and dynamin 2 on the specific uptake of [^{3}H]AEA. We were surprised to find that neither the β2 subunit of the AP2 complex nor dynamin 2 knockdown displayed any significant effect on the specific uptake of [^{3}H]AEA (Fig. 8). To explain the potentially conflicting result between [^{3}H]AEA and SKM 4-45-1 internalization, we hypothesized that dynamin 2 siRNA-transfected dCAD cells might be accumulating more [^{3}H]AEA at the plasma membrane instead of internalizing the AEA. If this were true, then FAAH would be unable to metabolize the [^{3}H]AEA that has been retained at the plasma membrane. Such an effect would be revealed by an increase in intact [^{3}H]AEA in the dynamin 2 siRNA-transfected cells after a 5-min uptake assay.

dCAD cells transfected with either mock or dynamin 2 siRNA were treated with [^{3}H]AEA for 5 min in the presence or absence of AM404. After [^{3}H]AEA treatment, each treatment group of cells was lysed, and the lipids were extracted using chloroform/methanol. TLC was performed on the lipid

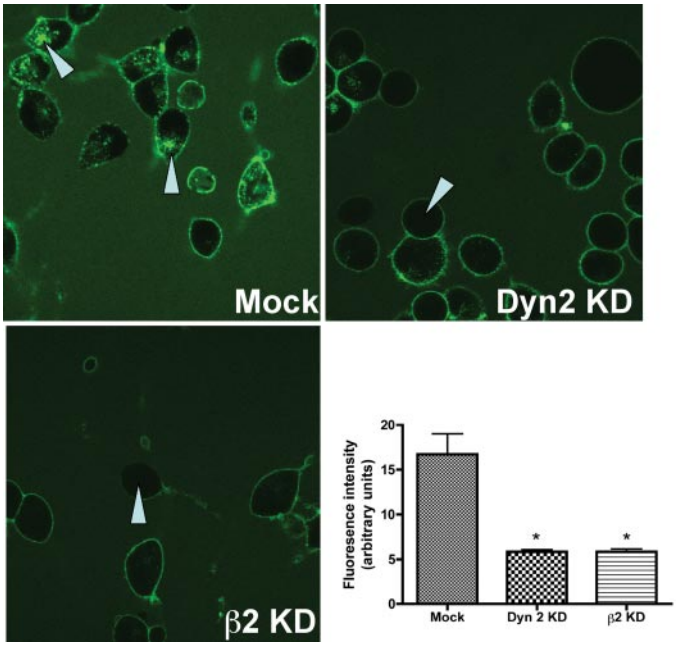

Fig. 5. Effect of RNAi knockdown of dynamin 2 and the β2 subunit of the AP2 complex on the internalization of 488-Tf in dCAD cells. Seventy-two hours after transfection with either mock, β2 subunit, or dynamin 2 siRNA, dCAD cells were incubated with 488-Tf for 10 min and imaged by confocal microscopy. Both β2 subunit- and dynamin 2 siRNA-transfected cells showed a reduction of 488-Tf internalization (indicated by arrows) compared with mock-transfected dCAD cells. Images were obtained using confocal microscopy as described under *Materials and Methods*. The internal fluorescence intensity of the intracellular space of all cells in the field of view was quantified using MetaMorph software (Molecular Devices, Sunnyvale, CA) (bottom right). Fifteen to 20 cells per experiment were analyzed. Data are representative of three separate experiments. Asterisks denote a significant difference in intracellular mean internal fluorescence intensity compared with mock-transfected cells (analysis of variance and Dunnett's multiple comparison test; $p < 0.01$).

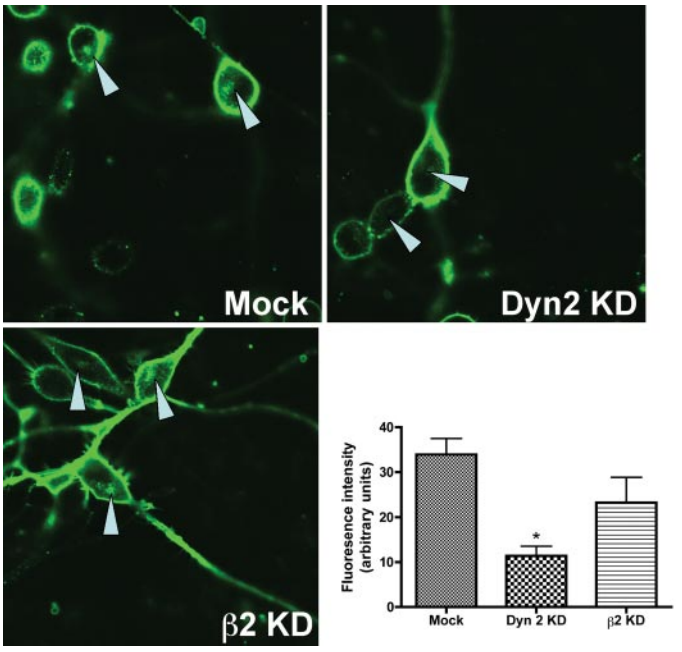

Fig. 6. Effect of RNAi knockdown of dynamin 2 and the β2 subunit of the AP2 complex on the internalization of 488-CT in dCAD cells. Seventy-two hours after transfection with either mock, β2 subunit, or dynamin 2 siRNA, dCAD cells were incubated with 488-CT for 10 min and imaged by confocal microscopy. Dynamin 2 siRNA-transfected cells showed a reduction of 488-CT internalization (indicated by arrows) compared with mock-transfected dCAD cells. β2 subunit siRNA-transfected cells did not display any difference in 488-CT internalization compared with mock-transfected dCAD cells, confirming the specificity of the treatments. Images were obtained using confocal microscopy as described under *Materials and Methods*. The internal fluorescence intensity of the intracellular space of all cells in the field of view was quantified using MetaMorph software (bottom right). Fifteen to 20 cells per experiment were analyzed. Data are representative of three separate experiments. Asterisks denote a significant difference in intracellular mean fluorescence intensity compared with mock-transfected cells (analysis of variance and Dunnett's multiple comparison test; $p < 0.05$).

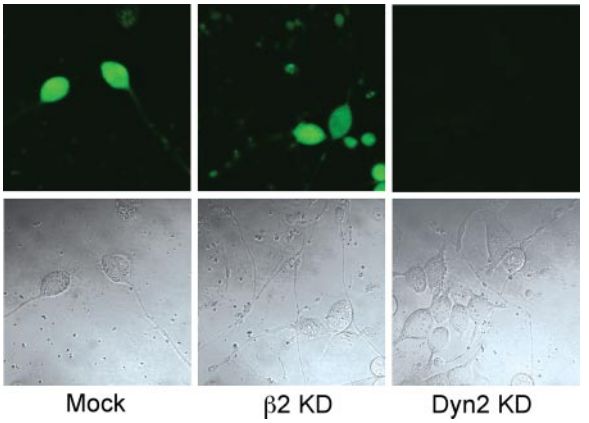

Fig. 7. SKM 4-45-1 internalization by dCAD cells after siRNA transfection. dCAD cells were treated with SKM 4-45-1 (25 μM) for 10 min at 72 h after transfection with mock, β2 subunit, or dynamin 2 siRNA. Knockdown of the β2 subunit of the AP2 complex had no effect on the SKM 4-45-1-derived fluorescence signal compared with mock. Knockdown of dynamin 2 in dCAD cells significantly decreased the accumulation of SKM 4-45-1-derived fluorescence. Images were obtained using confocal microscopy as described under *Materials and Methods*. Phase contrast images are shown below each corresponding fluorescence image. Data are representative of three separate experiments.

samples of each treatment group, and the levels of intact [^{3}H]AEA were quantified by scintillation counting. TLC analysis revealed that the specific levels of intact [^{3}H]AEA were approximately 2-fold higher in dCAD cells in which dynamin 2 had been knocked down compared with mock-transfected dCAD cells (Fig. 9A).

One explanation for the above-mentioned results could be that the knockdown of dynamin 2 altered FAAH activity. Examination of FAAH protein by Western blot analysis (Fig. 9B) and FAAH activity (Fig. 9C) after dynamin 2 knockdown indicated that the dynamin 2 knockdown had no detectable effect on FAAH. The lack of effect on FAAH and actin levels also confirms the specificity of our dynamin 2 siRNA (Fig. 9B).

Discussion

dCAD cells represent a biochemically and morphologically neuronal cell line that rapidly accumulates the endocannabinoid AEA and displays robust FAAH activity. Thus, dCAD cells may present a novel system useful in the study of endocannabinoid biosynthesis and inactivation.

Pharmacological inhibition of endocytosis in RBL-2H3 cells suggests that an endocytic process is involved in AEA uptake and that this process is clathrin-independent, potentially involving detergent-resistant membrane microdomains such as lipid rafts (McFarland et al., 2004). Our present results confirm these findings in the neuronal dCAD cell line as well. Pretreatment with nystatin/progesterone to disrupt detergent-resistant membrane microdomains significantly reduced the specific uptake of [^{3}H]AEA by dCAD cells by ~50%. An alternative explanation for our results with nystatin/progesterone could be that the treatment is generally toxic to the cells. Because a major factor determining nonspecific uptake relates to cell number, it is unlikely that the brief treatments caused a decrease in cell viability because nonspecific uptake of AEA was unaltered by the treatment (data not shown). We recognize that there is a lack of specificity associated with the chemical disruption of lipid rafts. Thus, a means of specifically disrupting endocytic processes without causing the potential nonspecific effects associated with the chemical disruption of lipid rafts was needed to assess the role that endocytosis may play in the cellular uptake of AEA.

The β2 subunit of the AP2 complex allows for the association of this complex with clathrin and is necessary for clathrin-mediated endocytosis to occur (Huang et al., 2004). Transferrin is internalized by a clathrin-mediated endocytic process (Johannes and Lamaze, 2002). As expected, RNAi knockdown of the β2 subunit of the AP2 complex inhibited transferrin internalization in dCAD cells but did not disrupt

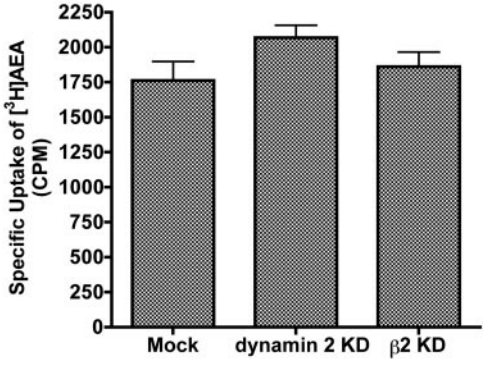

Fig. 8. [^{3}H]AEA uptake by dCAD cells after siRNA transfection. Seventy-two hours after transfection with mock, dynamin 2, or β2 subunit siRNA, [^{3}H]AEA uptake assays were performed in 1× KRH at 37°C as described under *Materials and Methods*. AM404 (100 μM) was used to define nonspecific transport. Data represent mean ± S.E.M. for three separate experiments performed in triplicate. The cpm values for mock cells were total = 2887 ± 136 and nonspecific = 1125 ± 128. The cpm values for dynamin 2 knockdown cells were total = 2973 ± 89 and nonspecific = 905 ± 83. The cpm values for β2 subunit knockdown cells were total = 2638 ± 104 and nonspecific = 777 ± 27.

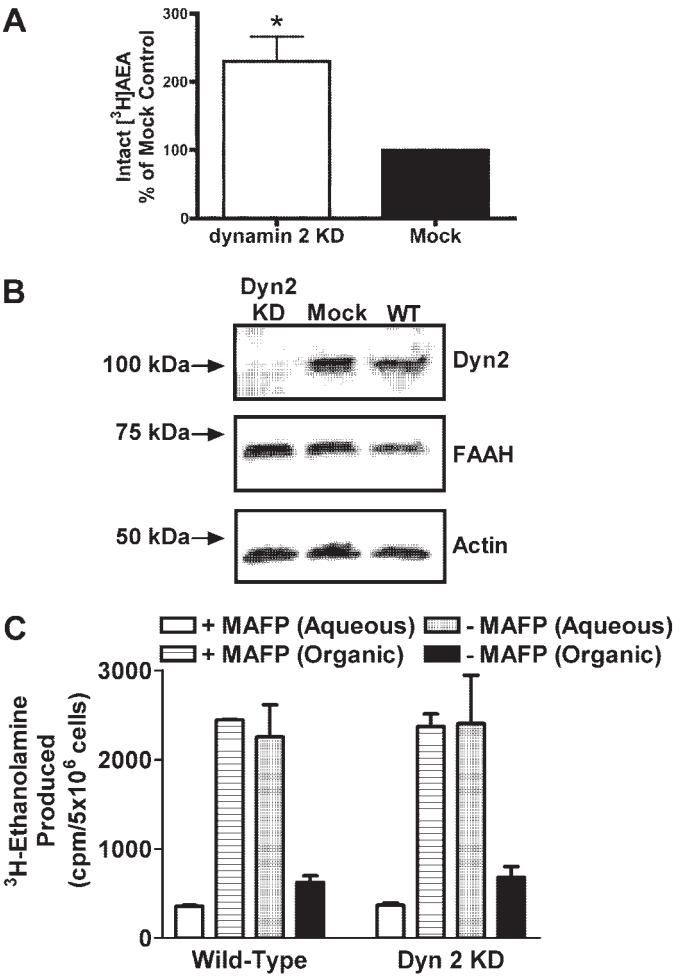

Fig. 9. Metabolism of [^{3}H]AEA in dynamin 2 siRNA-transfected dCAD cells. A, 72 h after transfection with either mock or dynamin 2 siRNA, dCAD cells were treated with [^{3}H]AEA for 5 min and then lysed. Cellular lipids were extracted from the cell lysates using chloroform/methanol and analyzed by TLC for intact [^{3}H]AEA. Nonspecific uptake was determined using 100 μM AM404. The graph represents data from three separate experiments. Statistical analysis was performed using a one-sample t test comparing with the value of 100 (mock control). *, $p < 0.05$. The cpm values from the TLC analysis for mock cells were total = 2986 ± 795 and nonspecific = 2243 ± 407. The cpm values from the TLC analysis for dynamin 2 knockdown cells were total = 3257 ± 545 and nonspecific = 1793 ± 198. B, FAAH expression after RNAi-mediated knockdown of dynamin 2. Knockdown of dynamin 2 in cCAD cells was performed as described under *Materials and Methods* except siLentFect Lipid Reagent (Bio-Rad) was used as the transfection reagent for 48 h with 10 nM siRNA oligo. Western blots were performed using the polyclonal dynamin 2 antibody, monoclonal FAAH antibody (1:1000; Abnova Corporation, Taipei City, Taiwan), monoclonal actin antibody (1:2000; Sigma-Aldrich, St. Louis, MO). C, FAAH activity after RNAi-mediated knockdown of dynamin 2. FAAH activity assays were performed on whole cell lysates as described under *Materials and Methods*. Data shown represent means ± S.D. from two experiments performed in quadruplicate.

the cellular accumulation of the cholera toxin B subunit or SKM 4-45-1, the fluorescently tagged analog of AEA. The cholera toxin B subunit is known to be internalized via a clathrin-independent (lipid raft-related) endocytic process (Johannes and Lamaze, 2002).

Whereas its role in neurons is not completely clear, the small GTPase dynamin 2 is probably involved in both clathrin-dependent and clathrin-independent endocytic recycling (Altschuler et al., 1998; Maxfield and McGraw, 2004). Thus, both transferrin and cholera toxin should require dynamin 2 expression for internalization to occur. RNAi knockdown of dynamin 2 significantly reduced both transferrin and cholera toxin accumulation by dCAD cells. Furthermore, dynamin 2 knockdown in dCAD cells inhibited the cellular internalization of SKM 4-45-1. Because the fluorescence associated with SKM 4-45-1 is only observed after internalization of the compound, it can be used as a marker for actual uptake (Muthian et al., 2000). One caveat of using only [^{3}H]AEA uptake is that conventional uptake assays do not differentiate between the tritium bound to the cells or membranes and the AEA that is actually transported into the cells. Taken together, our data suggest that actual internalization of AEA by dCAD cells occurs via a clathrin-independent endocytic process. Furthermore, dynamin 2 seems to play a role in the cellular uptake of AEA by the neuronal dCAD cells. Internalization of the B subunit of cholera toxin occurs by a lipid raft-mediated endocytic process (Johannes and Lamaze, 2002). Dynamin 2 knockdown significantly reduced 488-CT internalization in dCAD cells consistent with this dynamin 2-dependent, clathrin-independent endocytic process involving detergent-resistant membrane microdomains. An alternative approach to the knockdown of dynamin 2 or the β subunit of the AP2 complex could be to use siRNA targeted to clathrin itself. We were concerned about potential membrane effects reported with clathrin knockdowns and as such, we opted to focus on proteins downstream of clathrin in the endocytic pathways (Hinrichsen et al., 2003, 2006).

Dynamin 2 knockdown displayed a profound inhibitory effect on SKM 4-45-1 internalization in dCAD cells, and yet it did not have any observable effect on the specific uptake of [^{3}H]AEA. This discrepancy may be reconciled with the observation that [^{3}H]AEA uptake assays cannot discriminate between [^{3}H]AEA that has actually been internalized and [^{3}H]AEA that is binding to a target on the plasma membrane. Interestingly, a study conducted by Schmid and colleagues showed that expression of dominant-negative mutants of dynamin proteins inhibited endocytic processes but had no effect on endosomal recycling of membrane components to the cell surface (Altschuler et al., 1998). dCAD cells that have lost functioning dynamin 2 protein during the 72-h incubation after transfection with siRNA may be accumulating the AEA carrier in the detergent-resistant membrane microdomains. Precedence for such an effect comes from studies showing that expression of dominant-negative dynamin 2 mutant causes an accumulation of transferrin receptor at the cell surface (Altschuler et al., 1998). A similar phenomenon could be occurring with the putative AEA carrier after dynamin 2 knockdown. The accumulation of detergent-resistant membrane components at the cell surface with dynamin 2 knockdown could create a scenario in which dCAD cells, although they are not internalizing [^{3}H]AEA, are accumulating [^{3}H]AEA at the membrane. This effect would be due to more [^{3}H]AEA being able to associate with the plasma membrane that is now enriched with the putative carrier protein. This experimental limitation is not an issue in the case of SKM 4-45-1 internalization assays. Fluorescence from SKM 4-45-1 is not observed until after the compound is transported into the cell, and the fluorescent component of the molecule is liberated by esterases in the cell (Muthian et al., 2000). Thus, excess SKM 4-45-1 bound only at the membrane is not detectable.

We propose that knockdown of dynamin 2 in dCAD cells causes an accumulation of the AEA carrier in detergent-resistant membrane domains at the cell surface. There is no observable difference between the [^{3}H]AEA uptake in mock siRNA-transfected and dynamin 2 siRNA-transfected dCAD cells because more [^{3}H]AEA is able to associate with the plasma membrane carrier in the dynamin 2 siRNA-transfected cells. If this is true, then the majority of the radioactivity obtained from the dynamin 2 siRNA-transfected cells should be represented by intact [^{3}H]AEA. This is because AEA that is only associating with the cell surface and is not internalized will not be available to FAAH for metabolism. Indeed, TLC analysis of lipid extracts from dynamin 2 siRNA-transfected dCAD cells that were treated with [^{3}H]AEA for 5 min revealed levels of intact [^{3}H]AEA that were 2-fold greater than the levels of [^{3}H]AEA extracted from mock siRNA-transfected dCAD cells treated in the same manner. Furthermore, our results indicate that dynamin 2 knockdown does not alter FAAH protein or activity. These data support the hypothesis that dynamin 2 siRNA-transfected dCAD cells are able to accumulate more [^{3}H]AEA on their cell surface than mock-transfected dCAD cells due to an enrichment of the putative AEA carrier in the microdomains. If this is the case, then [^{3}H]AEA uptake assays may not be an ideal method for characterizing AEA internalization after the knockdown of proteins, such as dynamin 2, that are important in recycling events that maintain the composition of the plasma membrane. One alternative explanation for our results involves a possible role for the CB1 cannabinoid receptor in the uptake process. CB1 receptors have been shown to signal through lipid raft domains (Bari et al., 2005); thus, binding to CB1 receptors and subsequent internalization would be one possible mechanism for AEA uptake.

Unlike RBL-2H3 cells, we do not expect that dCAD cells contain caveolin-1, but we have preliminary evidence that dCAD cells express caveolin-3 (data not shown). Thus, caveolae-related endocytic processes may still be present in neurons and are dependent on intact detergent-resistant membrane microdomains. In summary, our data, combined with previous experiments in RBL-2H3 cells (McFarland et al., 2004), offer evidence that endocannabinoids are internalized by a lipid raft- or caveolae-related endocytic process. We speculate that the yet unidentified anandamide transporter will in fact be enriched in lipid rafts and functionally participate in endocytosis.

Acknowledgments

We thank Jason Parish for helpful discussion and technical assistance regarding TLC analysis of intact [^{3}H]AEA and the Purdue Cytomics Laboratory for technical assistance with microscopic imaging.

References

Altschuler Y, Barbas SM, Terlecky LJ, Tang K, Hardy S, Mostov KE, and Schmid SL (1998) Redundant and distinct functions for dynamin-1 and dynamin-2 isoforms. *J Cell Biol* **143:**1871–1881.

Bari M, Battista N, Fezza F, Finazzi-Agro A, and Maccarrone M (2005) Lipid rafts control signaling of type-1 cannabinoid receptors in neuronal cells. *J Biol Chem* **280:**12212–12220.

Cameron PL, Ruffin JW, Bollag R, Rasmussen H, and Cameron RS (1997) Identification of caveolin and caveolin-related proteins in the brain. *J Neurosci* **17:**9520–9535.

Cravatt BF, Giang DK, Mayfield SP, Boger DL, Lerner RA, and Gilula NB (1996) Molecular characterization of an enzyme that degrades neuromodulatory fatty-acid amides. *Nature* **384:**83–87.

Day TA, Rakhshan F, Deutsch DG, and Barker EL (2001) Role of fatty acid amide hydrolase in the transport of the endogenous cannabinoid anandamide. *Mol Pharmacol* **59:**1369–1375.

Deutsch DG and Chin SA (1993) Enzymatic synthesis and degradation of anandamide, a cannabinoid receptor agonist. *Biochem Pharmacol* **46:**791–796.

Di Marzo V, Bisogno T, and De Petrocellis L (2001) Anandamide: some like it hot. *Trends Pharmacol Sci* **22:**346–349.

Di Marzo V, Fontana A, Cadas H, Schinelli S, Cimino G, Schwartz JC, and Piomelli D (1994) Formation and inactivation of endogenous cannabinoid anandamide in central neurons. *Nature* **372:**686–691.

Glaser ST, Abumrad NA, Fatade F, Kaczocha M, Studholme KM, and Deutsch DG (2003) Evidence against the presence of an anandamide transporter. *Proc Natl Acad Sci U S A* **100:**4269–4274.

Hashemi SH, Li JY, Faigle R, and Dahlstrom A (2003) Adrenergic differentiation and SSR2(a) receptor expression in CAD-cells cultured in serum-free medium. *Neurochem Int* **42:**9–17.

Hinrichsen L, Harborth J, Andrees L, Weber K, and Ungewickell EJ (2003) Effect of clathrin heavy chain- and α-adaptin-specific small inhibitory RNAs on endocytic accessory proteins and receptor trafficking in HeLa cells. *J Biol Chem* **278:**45160–45170.

Hinrichsen L, Meyerholz A, Groos S, and Ungewickell EJ (2006) Bending a membrane: how clathrin affects budding. *Proc Natl Acad Sci U S A* **103:**8715–8720.

Huang F, Khvorova A, Marshall W, and Sorkin A (2004) Analysis of clathrin-mediated endocytosis of epidermal growth factor receptor by RNA interference. *J Biol Chem* **279:**16657–16661.

Johannes L and Lamaze C (2002) Clathrin-dependent or not: is it still a question? *Traffic* **3:**443–451.

Lazaroff M (1996) A CNS catecholaminergic cell line expresses voltage-gated currents. *J Membr Biol* **151:**279–291.

Lazaroff M, Qi Y, and Chikaraishi DM (1998) Differentiation of a catecholaminergic CNS cell line modifies tyrosine hydroxylase transcriptional regulation. *J Neurochem* **71:**51–59.

Matsuda LA, Lolait SJ, Brownstein MJ, Young AC, and Bonner TI (1990) Structure of a cannabinoid receptor and functional expression of the cloned cDNA. *Nature* **346:**561–564.

Maxfield FR and McGraw TE (2004) Endocytic recycling. *Nat Rev Mol Cell Biol* **5:**121–132.

McFarland MJ, Porter AC, Rakhshan F, Rawat DS, Gibbs RA, and Barker EL (2004) A role for caveolae/lipid rafts in the uptake and recycling of the endogenous cannabinoid anandamide. *J Biol Chem* **279:**41991–41997.

Millard EE, Gale SE, Dudley N, Zhang J, Schaffer JE, and Ory DS (2005) The sterol-sensing domain of the Niemann-Pick C1 (NPC1) protein regulates trafficking of low density lipoprotein cholesterol. *J Biol Chem* **280:**28581–28590.

Munro S, Thomas KL, and Abu-Shaar M (1993) Molecular characterization of a peripheral receptor for cannabinoids. *Nature* **365:**61–65.

Muthian S, Nithipatikom K, Campbell WB, and Hillard CJ (2000) Synthesis and characterization of a fluorescent substrate for the *N*-arachidonoylethanolamine (anandamide) transmembrane carrier. *J Pharmacol Exp Ther* **293:**289–295.

Qi Y, Wang JK, McMillian M, and Chikaraishi DM (1997) Characterization of a CNS cell line, CAD, in which morphological differentiation is initiated by serum deprivation. *J Neurosci* **17:**1217–1225.

Suri C, Fung BP, Tischler AS, and Chikaraishi DM (1993) Catecholaminergic cell lines from the brain and adrenal glands of tyrosine hydroxylase-SV40 T antigen transgenic mice. *J Neurosci* **13:**1280–1291.

Voets T and Nilius B (2003) TRPs make sense. *J Membr Biol* **192:**1–8.

Wang H and Oxford GS (2000) Voltage-dependent ion channels in CAD cells: a catecholaminergic neuronal line that exhibits inducible differentiation. *J Neurophysiol* **84:**2888–2895.

Address correspondence to: Dr. Eric L. Barker, Department of Medicinal Chemistry and Molecular Pharmacology, Purdue University, 575 Stadium Mall Dr., West Lafayette, IN 47907-2091. E-mail: ericb@pharmacy.purdue.edu